2015

On the presence of giant particles downwind of ships in the marine boundary layer

Sorooshian, Armin; Prabhakar, Gouri; Jonsson, Haflidi; Woods, Roy K.; Flagan, Richard C.; Seinfeld, John H.

AGU Publications

On the presence of giant particles downwind of ships in the marine boundary layer

Armin Sorooshian[1,2], Gouri Prabhakar[2,3], Haflidi Jonsson[4], Roy K. Woods[4], Richard C. Flagan[5], and John H. Seinfeld[5]

[1]Department of Chemical and Environmental Engineering, University of Arizona, Tucson, Arizona, USA, [2]Department of Atmospheric Sciences, University of Arizona, Tucson, Arizona, USA, [3]Now at Department of Civil and Environmental Engineering, University of California, Davis, California, USA, [4]Naval Postgraduate School, Monterey, California, USA, [5]Department of Chemical Engineering, California Institute of Technology, Pasadena, California, USA

Abstract This study examines large oceangoing ships as a source of giant cloud condensation nuclei ($D_p > 2\,\mu m$) due to wake and stack emissions off the California coast. Observed particle number concentrations behind 10 ships exceeded those in "control" areas, exhibiting number concentration enhancement ratios (ERs) for minimum threshold diameters of ~2, ~10, and ~20 μm as high as 2.7, 5.5, and 7.5, respectively. ER decreases with increasing downwind distance and altitude. ER becomes better correlated with ship size variables (gross tonnage, length, and beam) as the minimum size threshold increases from 2 to 20 μm, whereas ship speed has a less distinct relationship with ER. One case study of a container ship shows that there are higher concentrations of sea-salt tracer species behind it relative to adjacent control areas. These results have implications for cloud properties and precipitation in marine boundary layers exposed to ship traffic.

1. Introduction

Oceangoing ships are a source of aerosol particles due to both their wake and stack emissions. Ship stack emissions have received the majority of the attention owing to their influence on air quality, radiative forcing, and microphysical properties of aerosol particles and clouds [e.g., *Capaldo et al.*, 1999; *Corbett et al.*, 2007; *Fuglestvedt et al.*, 2009; *Eyring et al.*, 2010; *Partanen et al.*, 2013]. The increase in the number of cloud condensation nuclei (CCN) from ship exhaust is linked to brightened clouds ("ship tracks") and suppression of warm rain (at fixed cloud liquid water content) [e.g., *Ferek et al.*, 2000; *Lu et al.*, 2009]. Giant CCN (GCCN), commonly defined as being particles with diameters exceeding 2 μm [*Yin et al.*, 2000], are thought to have a contrasting effect on warm clouds as they can accelerate the broadening of the cloud drop distribution and production of precipitation in boundary layer clouds [e.g., *Johnson*, 1982; *Szumowski et al.*, 1999; *Rudich et al.*, 2002; *Jensen and Lee*, 2008; *L'Ecuyer et al.*, 2009; *Kogan et al.*, 2012; *Sorooshian et al.*, 2013a; *Jung et al.*, 2015] with their largest influence being in cases with high CCN concentrations [e.g., *Feingold et al.*, 1999]. The potential of aerosol particles to affect cloud properties, and thereby impact climate, is especially important in the case of stratocumulus clouds that have bases close to the ocean surface and ships. Additionally, cloud water influenced by emissions associated with ships exhibits enhanced levels of species that can alter chemical kinetics in droplets and affect ecosystems after wet deposition [e.g., *Coggon et al.*, 2012; *Hassellov et al.*, 2013; *Sorooshian et al.*, 2013b; *Prabhakar et al.*, 2014; *Wang et al.*, 2014].

Most observational studies have focused on particulate emissions with diameters below roughly 1–2 μm from marine vessels [e.g., *Petzold et al.*, 2008, 2010; *Juwono et al.*, 2013; *Russell et al.*, 2013; *Cappa et al.*, 2014]. One field experiment examining larger particles, the Monterey Area Ship Track (MAST) experiment in June 1994, identified no recognizable signature of water-wake particles via both size distribution and chemical analysis and concluded that wake particles do not contribute to ship track formation [*Durkee et al.*, 2000]. Alternatively, *Feingold et al.* [1999] suggested that while the number concentration of small particles emitted in the wake of ships is too low to increase cloud albedo, even very low concentrations of larger GCCN emitted in the wake can reduce cloud albedo by enhancing collision-coalescence.

The goal of this study is to revisit the question of whether giant particles are emitted by the action of ships (i.e., stack and wake emissions) using measurements on an airborne platform that conducted strategic flight patterns at low altitude and within close proximity to 10 different ships of varying dimensions and speeds. This study also aims to identify factors influencing potential GCCN number concentration enhancements

behind ships. In contrast to MAST, the relevance of the results of this study shifts from being focused on ship track formation to the effects on expedited drop collision-coalescence and precipitation production in low-level stratocumulus clouds.

2. Experimental Methods

Data are analyzed from three flight campaigns using the Center for Interdisciplinary Remotely-Piloted Aircraft Studies Twin Otter off the California coast. The second Marine Stratus/Stratocumulus Experiment (MASE II) [*Lu et al.*, 2009] included 16 research flights in July 2007, the Eastern Pacific Emitted Aerosol Cloud Experiment (E-PEACE) [*Russell et al.*, 2013] included 30 flights between July and August in 2011, and the Nucleation in California Experiment (NiCE) included 23 flights between July and August in 2013 [*Coggon et al.*, 2014].

The Twin Otter carried a nearly identical assembly of instruments in these experiments measuring physical and chemical properties of particles and clouds. This study focuses on aerosol measurements below cloud base or in clear air on cloud-free days. Clear air is identified as having liquid water content values below $0.01 \, \mathrm{g \, m^{-3}}$, as detected by a PVM-100 probe [*Gerber et al.*, 1994]; relative humidities in our cases were below 97.5% (Table 1). Particle number concentrations in the different size ranges were observed with a condensation particle counter (CPC 3010; TSI Inc.; $D_p > 10 \, \mathrm{nm}$), passive cavity aerosol spectrometer probe (PCASP; $D_p \sim 0.1$–$2.6 \, \mu\mathrm{m}$), and cloud aerosol spectrometer (CAS; $D_p \sim 0.6$–$60 \, \mu\mathrm{m}$). These data have 1 s time resolution, which corresponds to 50 m spatial resolution as the Twin Otter typically flew at $50 \, \mathrm{m \, s^{-1}}$. Three minimum size thresholds used for grouping GCCN are approximately 2, 10, and $20 \, \mu\mathrm{m}$. GCCN data are obtained only from the CAS in this study, whereas the CPC and PCASP are used as plume markers. Threshold sizes exceeding $20 \, \mu\mathrm{m}$ (such as 30 and $40 \, \mu\mathrm{m}$) are not used since number concentrations were zero for at least half of the cases examined above those sizes. Water-soluble $PM_{2.5}$ composition data are reported for a case study in MASE II using a particle-into-liquid sampler (PILS, Brechtel Manufacturing Inc.) coupled to ion chromatography [*Sorooshian et al.*, 2006].

Ten cases are studied from nine research flights (RFs), which offer sufficient statistics behind ships at low altitudes ($<150 \, \mathrm{m}$) both in areas affected by ships and those unaffected (control areas). Ship-influenced areas are identified based on the number concentration data from the PCASP and CPC, which usually increased by an order of magnitude in the plume relative to outside of the plume where concentrations were usually below $500 \, \mathrm{cm^{-3}}$ as measured by both instruments. In relation to each other, control and ship-influenced areas were typically within 5 m altitude, $1.5 \, \mathrm{m \, s^{-1}}$ of wind speed, and 2% relative humidity (Table 1). The influence of potential ship wake emissions is expected to be found within the plume measurements (and not in control areas) at the close distances flown behind the ships, as will be chemically supported subsequently. Information about the ships' physical dimensions and speeds were obtained from a marine traffic source (https://www.marinetraffic.com/en/). Each of the RFs tracked a moving ship either in straight legs in the plume ("racetracks") or in crosswind transects behind the ship ("zigzags") as illustrated in Figure 1. The measurements were made within approximately 5 km (most within ~1 km) behind the ships.

3. Results and Discussion

3.1. GCCN Enhancement Behind Ships

The 10 ships examined are categorized as container (7), tanker (2), and bulk carrier (1), with gross tonnage (GT) ranging from 19,707 to 131,332 and speeds reported between 6.6 and $11.8 \, \mathrm{m \, s^{-1}}$ (Table 1). GT is positively correlated (r^2) with the other physical ship variables for the 10 cases: length (0.80), beam (0.78), deadweight tonnage (0.73), and draught (0.45). While numerous passes were made behind ships in some flights, Table 1 reports particle concentration data for only the strongest signature of the plume in each flight, as represented by average PCASP concentrations behind ships. (Note that the CPC was often saturated in ship plumes and thus comparing average concentrations is not meaningful.) Each case was characterized by enhanced GCCN concentrations behind ships for the $2 \, \mu\mathrm{m}$ diameter threshold, with an enhancement ratio (ER = ship:control number concentration ratio) ranging from 1.02 to 2.71 (average = 1.50). The average ERs for the 10 and $20 \, \mu\mathrm{m}$ thresholds were 2.12 and 3.03, respectively. The difference between the mean GCCN concentration behind ships and control areas was statistically significant to 95% confidence (using a two-sample t test) for between four and six ships for the three size thresholds; many of the other cases did

Table 1. Summary of Characteristics for 10 Ships Studied in Nine Research Flights[a]

		Ships						Twin Otter							
Case	Type	Length (m)	Beam (m)	Deadweight Tonnage	Gross Tonnage	Draught (m)	Speed (m s⁻¹)	Air Type	Alt (m)	Wind (m s⁻¹)	RH (%)	PCASP (cm⁻³)	CAS-2 (cm⁻³)	CAS-10 (cm⁻³)	CAS-20 (cm⁻³)
MASE II RF6	Container	347	43	110,387	91,690	12.4	11.3	Ship	28	9.7	93.6	4,394	**3.72**	**0.27**	**0.04**
								Control	32	10.5	93.2	317	2.18	0.09	0.00
E-PEACE RF5	Tanker	228	33	63,589	38,997	9.7	7.2	Ship	91	4.8	96.0	1,519	**1.12**	0.07	0.02
								Control	88	5.1	97.4	22	0.76	0.10	0.02
E-PEACE RF11	Container	276	32	47,539	48,305	8.0	8.5	Ship	82	4.0	89.9	1,571	4.49	0.19	**0.04**
								Control	71	3.9	90.4	327	4.40	0.13	0.02
E-PEACE RF12	Bulk Carrier	171	27	13,949	19,707	7.8	6.6	Ship	42	1.9	84.9	1,163	0.91	0.01	0.00
								Control	37	2.3	82.9	338	0.72	0.02	0.00
E-PEACE RF13	Tanker	274	48	158,070	84,029	13.2	7.0	Ship	77	10.6	93.2	2,955	**3.32**	**0.31**	**0.13**
								Control	79	11.8	92.6	90	2.48	0.16	0.05
E-PEACE RF24	Container	294	32	63,292	54,005	13.5	11.6	Ship	75	6.1	88.1	1,089	**5.37**	0.16	0.03
								Control	74	5.0	88.4	194	4.74	0.11	0.02
E-PEACE RF25	Container	300	40	81,171	75,484	11.7	11.8	Ship	62	7.6	94.8	4,444	**0.93**	**0.25**	**0.13**
								Control	59	7.6	95.3	29	0.34	0.09	0.08
NiCE RF2	Container	363	46	128,550	131,332	12.2	7.7	Ship	52	6.7	95.4	2,598	**1.77**	**0.08**	**0.03**
								Control	50	6.4	95.5	302	1.10	0.01	0.00
NiCE RF11A	Container	267	35	52,184	44,234	11.0	10.7	Ship	80	3.1	96.0	2,022	2.15	0.12	0.00
								Control	81	4.8	96.0	124	1.58	0.04	0.00
NiCE RF11B	Container	221	35	45,349	37,199	8.9	11.3	Ship	87	5.2	96.0	2,078	1.35	0.03	0.00
								Control	85	3.8	96.7	80	1.00	0.02	0.01

[a]To the right is a summary of environmental properties and average number concentrations of GCCN ($D_p > 2$, 10, and 20 μm), measured by the CAS probe, behind each ship ("ship") and in adjacent "control" areas. Values in bold indicate when the difference of the mean between the ship and control areas is statistically significant at the 95% confidence level using a two-sample t test.
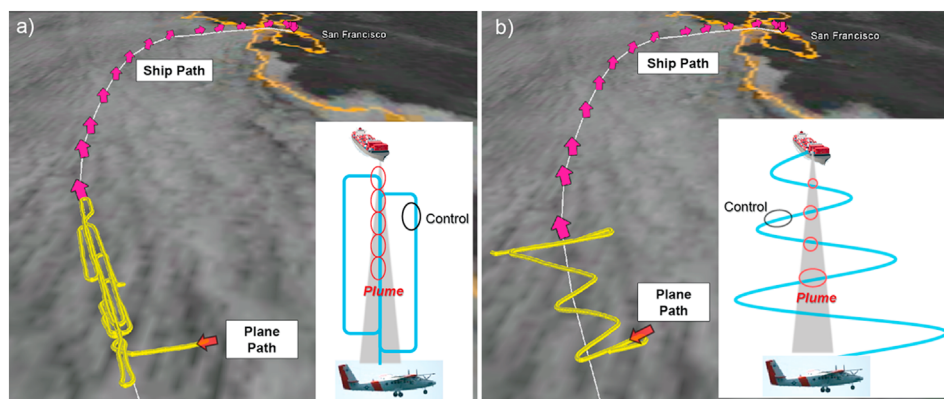
Figure 1. Representative flight paths during E-PEACE RF25 for the two main strategies used to study ship emissions: (a) racetrack patterns and (b) zigzag patterns. "Ship path" corresponds to the container ship being studied (details in Table 1) that was moving toward the San Francisco area. GOES-15 visible satellite imagery during the flight shows the presence of low-lying stratocumulus clouds.

not reach this criteria owing to limited data points in close proximity to the rear of ships and thus suffered from the nature of the measurements.

GCCN emitted by ships have the potential to impact cloud properties if entrained into cloud base. For instance, *Jung et al.* [2015] show that salt particles (D_p ~ 1–10 μm) with concentrations on the order of 10^{-2} to 10^{-4} cm^{-3} are sufficient to promote a fourfold increase in cloud base rainfall rate in the same study region. The average differences between ship and control areas for the 2, 10, and 20 μm size thresholds were 0.58 cm^{-3}, 0.07 cm^{-3}, and 0.02 cm^{-3}, respectively. These enhancements are especially significant since the ability of GCCN to enhance the collision-coalescence process is greatest when CCN concentrations are already high [*Feingold et al.*, 1999], as is the case downwind of ships. It is cautioned though that the measured concentrations likely are an overestimate of those expected to reach cloud base height and future work is needed to more directly make the link with clouds.

3.2. MASE II Case Study

RF6 from MASE II was a special case that allowed two hypotheses to be tested, specifically (i) that ER decreases with increasing altitude and downwind distance from ships and (ii) that concentrations of sea-salt tracer species are higher behind a ship relative to control areas due to wake emissions. This day involved one of the largest ships studied (GT = 91,690) moving at one of the fastest speeds (11.3 m s^{-1}) resulting in wide plume that could easily be followed by the Twin Otter (flight map in Figure S1 in the supporting information). This particular ship operated with a two-stroke, slow-speed diesel engine that was operated as 57% of maximum power using heavy fuel oil with properties discussed by *Murphy et al.* [2009]. PCASP and CAS number concentrations decreased with downwind distance (up to ~40 km away from ship) during a representative level leg at ~30 m altitude in the plume, regardless of the minimum size threshold (Figure S2 in the supporting information). Particle number concentrations also decreased with altitude, with the greatest reductions for the 20 μm minimum size threshold, which reached zero starting at ~60 m with its maximum value being 0.04 cm^{-3} at ~30 m, which was the lowest altitude reached in flight (Figure S3 in the supporting information).

The PILS-IC method (~4.5 min time resolution, this flight) was used to identify if water-soluble species known to be associated with sea-salt GCCN in the marine boundary layer (i.e., sodium and chloride) were enhanced behind the ship relative to control areas. Since at the lowest altitude (~30 m), there were no samples completely uninfluenced by the plume, samples in racetrack legs behind the ship are compared to samples in crosswind transects that represent far less time in ship-influenced areas. The average mass concentrations (μg m^{-3}) of Cl$^-$, Na$^+$, and SO$_4^{2-}$ were as follows (ship/control): 0.81/0.15 μg m^{-3}, 1.77/0.25 μg m^{-3}, and 54.33/3.10. The enhancements in Cl$^-$ and Na$^+$ exceeded a factor of 5, due most likely to wake emissions. The reduced Cl$^-$:Na$^+$ mass ratio as compared to natural sea salt (1.8) is most likely due to chloride depletion from acidic species derived from precursors in ship exhaust such as nitric and sulfuric acids. While wake emissions are shown to enhance GCCN concentrations, this is likely concomitant with contributions from stack emissions since ship

Table 2. Correlation (*r*) Matrix Between the GCCN Number Concentration Enhancement Ratio (Ship:Control) and Influential Factors[a]
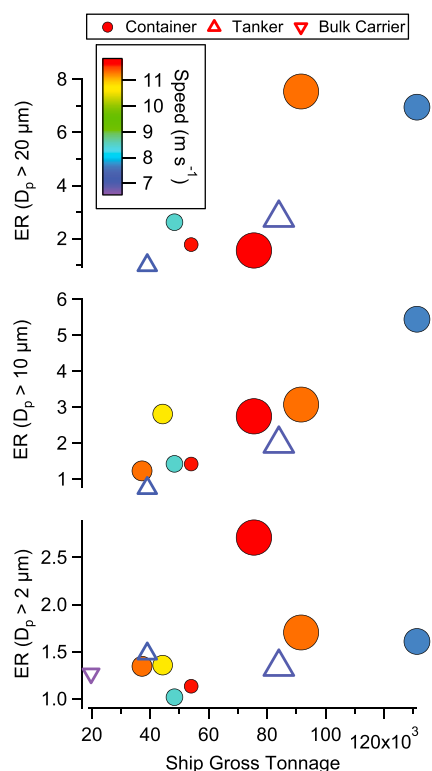
Ship Type	D_p (μm) Threshold	Ships						Twin Otter	
		Length	Beam	DWT	GT	Draught	Speed	Altitude	PCASP
All	2	0.33	0.39	0.25	0.37	0.28	0.37	−0.31	**0.79**
	10	**0.86**	**0.74**	**0.63**	**0.90**	0.55	0.17	−0.37	**0.59**
	20	**0.87**	0.60	0.52	**0.80**	0.27	0.04	**−0.86**	0.50
Container	2	0.30	0.56	0.41	0.38	0.31	0.34	−0.44	**0.85**
	10	**0.79**	**0.88**	**0.87**	**0.91**	0.44	−0.51	−0.61	0.48
	20	**0.90**	0.78	0.84	0.78	0.21	−0.36	−0.82	0.42

[a]DWT = deadweight tonnage, GT = gross tonnage. Values in bold are statistically significant at 95% with a two-tailed student's *t* test.

engine exhaust studies have shown that coarse-sized particles are emitted [e.g., *Lyyranen et al.*, 1999; *Winnes and Fridell*, 2009]. Such GCCN are sufficiently large to activate into drops regardless of their chemical and hygroscopic nature in the marine boundary layer [*Russell et al.*, 2013; *Wonaschütz et al.*, 2013].

3.3. Factors Influencing GCCN Concentrations Behind Ships

Previous work has studied the sensitivity of physicochemical properties of particles to fuel sulfur content, engine type, and vessel activity, but mainly for the submicrometer size range [e.g., *Lack et al.*, 2009; *Jonsson et al.*, 2011; *Buffaloe et al.*, 2014; *Cappa et al.*, 2014; *Anderson et al.*, 2015]. Table 2 reports correlation matrices for size-dependent ERs versus influential factors both for all ships and for only container ships as an attempt to hold ship type fixed. The strongest correlative factor with ER for the 2 μm threshold is PCASP concentration (*r* = 0.79 for all ships and *r* = 0.85 for container ships), due to some combination of stack emissions or small sea-salt generation in wakes. Aircraft altitude was negatively correlated with ER, with the strongest antirelationship for the 20 μm size threshold (*r* = −0.86 for all ships), due likely to the difficulty for the largest particles to be lofted to higher altitudes. For the two larger-diameter thresholds, ER is generally best correlated with ship physical characteristics such as length, beam, and GT. The ships with the lowest GT (19,707–44,234), which include the bulk carrier, the smallest tanker, and the two smallest container ships, exhibited ERs close to or below unity for the 20 μm threshold. Thus, larger ships are linked with greater emissions of larger GCCN. Ship speed exhibited a weak correlation with ER for all size thresholds presumably due to the small range of speeds encountered and the dominating effect of other factors examined such as GT, plume strength (i.e., PCASP concentration), and aircraft altitude (Figure 2).

In terms of ship type, container ships exhibited the highest ERs for all size thresholds, followed by tankers and finally the bulk carrier ship. However, the comparison of ship types cannot be untangled from other factors since the container (bulk carrier) ships also coincided with the highest (lowest) GTs, speeds, and PCASP concentrations.

4. Conclusions

This study uses airborne data off the California coast to show that there is an enhancement in GCCN number

Figure 2. GCCN number concentration enhancement ratio (ship:control) for three minimum size thresholds as a function of ship type, ship gross tonnage, ship speed, and plume strength (marker size ~ PCASP concentration, range: 1089–4444 cm^{-3}). Markers missing in the top two panels indicate no particles detected behind the ship above that particular minimum diameter threshold.

concentration behind oceangoing ships. At the point closest to each ship, the average number concentration difference between ship-affected and unaffected control areas for the 2, 10, and 20 μm minimum diameter thresholds was 0.58, 0.07, and 0.02 cm^{-3} (corresponding ER: 1.50, 2.12, and 3.03), respectively, which is sufficient to potentially impact cloud properties if entrained into cloud base. Factors leading to higher enhancements include lower altitudes, closer proximity to ships, stronger plumes (i.e., higher PCASP concentrations), and larger ships (e.g., length, beam, and gross tonnage), the latter of which is observed to be more important for the larger minimum threshold diameters (10 μm and 20 μm). Ship speed is not observed to be as strong a factor due to some likely combination of too narrow of a range of speeds encountered (6.6–11.8 m s^{-1}) and the dominant influence of other factors. A case study of one of the larger ships provides evidence for enhanced levels of sea-salt tracer species behind the ship relative to less perturbed control areas. Wake and stack emissions likely both contribute to the observed GCCN enhancements behind the ships studied, but future work should build more statistics to address the relative importance of wake versus stack emissions in contributing to GCCN as a function of aerosol size. Furthermore, studying more ships can help address the sensitivity of GCCN emissions to individual ship-related factors such as ship type, gross tonnage, engine type, and speed.

The results have implications for treatment of boundary layer clouds since the presence of GCCN emissions from ships can potentially affect cloud albedo and the timing of precipitation onset.

References

Anderson, M., K. Salo, A. M. Hallquist, and E. Fridell (2015), Characterization of particles from a marine engine operating at low loads, *Atmos. Environ.*, *101*, 65–71, doi:10.1016/j.atmosenv.2014.11.009.

Buffaloe, G. M., et al. (2014), Black carbon emissions from in-use ships: A California regional assessment, *Atmos. Chem. Phys.*, *14*(4), 1881–1896, doi:10.5194/acp-14-1881-2014.

Capaldo, K., J. J. Corbett, P. Kasibhatla, P. Fischbeck, and S. N. Pandis (1999), Effects of ship emissions on sulphur cycling and radiative climate forcing over the ocean, *Nature*, *400*(6746), 743–746, doi:10.1038/23438.

Cappa, C. D., et al. (2014), A case study into the measurement of ship emissions from plume intercepts of the NOAA ship Miller Freeman, *Atmos. Chem. Phys.*, *14*(3), 1337–1352, doi:10.5194/acp-14-1337-2014.

Coggon, M. M., et al. (2012), Ship impacts on the marine atmosphere: Insights into the contribution of shipping emissions to the properties of marine aerosol and clouds, *Atmos. Chem. Phys.*, *12*(18), 8439–8458, doi:10.5194/acp-12-8439-2012.

Coggon, M. M., A. Sorooshian, Z. Wang, J. S. Craven, A. R. Metcalf, J. J. Lin, A. Nenes, H. H. Jonsson, R. C. Flagan, and J. H. Seinfeld (2014), Observations of continental biogenic impacts on marine aerosol and clouds off the coast of California, *J. Geophys. Res. Atmos.*, *119*, 6724–6748, doi:10.1002/2013JD021228.

Corbett, J. J., J. J. Winebrake, E. H. Green, P. Kasibhatla, V. Eyring, and A. Lauer (2007), Mortality from ship emissions: A global assessment, *Environ. Sci. Technol.*, *41*(24), 8512–8518.

Durkee, P. A., et al. (2000), The impact of ship-produced aerosols on the microstructure and albedo of warm marine stratocumulus clouds: A test of MAST hypotheses 1i and 1ii, *J. Atmos. Sci.*, *57*(16), 2554–2569.

Eyring, V., I. S. A. Isaksen, T. Berntsen, W. J. Collins, J. J. Corbett, O. Endresen, R. G. Grainger, J. Moldanova, H. Schlager, and D. S. Stevenson (2010), Transport impacts on atmosphere and climate: Shipping, *Atmos. Environ.*, *44*(37), 4735–4771, doi:10.1016/j.atmosenv.2009.04.059.

Feingold, G., W. R. Cotton, S. M. Kreidenweis, and J. T. Davis (1999), The impact of giant cloud condensation nuclei on drizzle formation in stratocumulus: Implications for cloud radiative properties, *J. Atmos. Sci.*, *56*(24), 4100–4117.

Ferek, R. J., et al. (2000), Drizzle suppression in ship tracks, *J. Atmos. Sci.*, *57*(16), 2707–2728.

Fuglestvedt, J., T. Berntsen, V. Eyring, I. Isaksen, D. S. Lee, and R. Sausen (2009), Shipping emissions: From cooling to warming of climate-and reducing impacts on health, *Environ. Sci. Technol.*, *43*(24), 9057–9062.

Gerber, H., B. G. Arends, and A. S. Ackerman (1994), New microphysics sensor for aircraft use, *Atmos. Res.*, *31*(4), 235–252.

Hassellov, I. M., D. R. Turner, A. Lauer, and J. J. Corbett (2013), Shipping contributes to ocean acidification, *Geophys. Res. Lett.*, *40*, 2731–2736, doi:10.1002/grl.50521.

Jensen, J. B., and S. H. Lee (2008), Giant sea-salt aerosols and warm rain formation in marine stratocumulus, *J. Atmos. Sci.*, *65*(12), 3678–3694.

Johnson, D. B. (1982), The role of giant and ultragiant nuclei in warm rain initiation, *J. Atmos. Sci.*, *39*, 448–460.

Jonsson, A. M., J. Westerlund, and M. Hallquist (2011), Size-resolved particle emission factors for individual ships, *Geophys. Res. Lett.*, *38*, L13809, doi:10.1029/2011GL047672.

Jung, E., B. A. Albrecht, H. H. Jonsson, Y.-C. Chen, J. H. Seinfeld, A. Sorooshian, A. R. Metcalf, S. Song, M. Fang, and L. M. Russell (2015), Precipitation effects of giant cloud condensation nuclei artificially introduced into stratocumulus clouds, *Atmos. Chem. Phys. Discuss.*, *15*, 47–76, doi:10.5194/acpd-15-47-2015.

Juwono, A. M., G. R. Johnson, M. Mazaheri, L. Morawska, F. Roux, and B. Kitchen (2013), Investigation of the airborne submicrometer particles emitted by dredging vessels using a plume capture method, *Atmos. Environ.*, *73*, 112–123.

Kogan, Y. L., D. B. Mechem, and K. Choi (2012), Effects of sea-salt aerosols on precipitation in simulations of shallow cumulus, *J. Atmos. Sci.*, *69*(2), 463–483.

Lack, D. A., et al. (2009), Particulate emissions from commercial shipping: Chemical, physical, and optical properties, *J. Geophys. Res.*, *114*, D00F04, doi:10.1029/2008JD011300.

L'Ecuyer, T. S., W. Berg, J. Haynes, M. Lebsock, and T. Takemura (2009), Global observations of aerosol impacts on precipitation occurrence in warm maritime clouds, *J. Geophys. Res.*, *114*, D09211, doi:10.1029/2008JD011273.

Lu, M. L., A. Sorooshian, H. H. Jonsson, G. Feingold, R. C. Flagan, and J. H. Seinfeld (2009), Marine stratocumulus aerosol-cloud relationships in the MASE-II experiment: Precipitation susceptibility in eastern Pacific marine stratocumulus, *J. Geophys. Res.*, *114*, D24203, doi:10.1029/2009JD012774.

Lyyranen, J., J. Jokiniemi, E. I. Kauppinen, and J. Joutsensaari (1999), Aerosol characterisation in medium-speed diesel engines operating with heavy fuel oils, *J. Aerosol Sci.*, *30*(6), 771–784.

Murphy, S. M., et al. (2009), Comprehensive simultaneous shipboard and airborne characterization of exhaust from a modern container ship at sea, *Environ. Sci. Technol.*, *43*(13), 4626–4640.

Partanen, A. I., A. Laakso, A. Schmidt, H. Kokkola, T. Kuokkanen, J. P. Pietikainen, V. M. Kerminen, K. E. J. Lehtinen, L. Laakso, and H. Korhonen (2013), Climate and air quality trade-offs in altering ship fuel sulfur content, *Atmos. Chem. Phys.*, *13*(23), 12,059–12,071.

Petzold, A., J. Hasselbach, P. Lauer, R. Baumann, K. Franke, C. Gurk, H. Schlager, and E. Weingartner (2008), Experimental studies on particle emissions from cruising ship, their characteristic properties, transformation and atmospheric lifetime in the marine boundary layer, *Atmos. Chem. Phys.*, *8*(9), 2387–2403.

Petzold, A., E. Weingartner, I. Hasselbach, P. Lauer, C. Kurok, and F. Fleischer (2010), Physical properties, chemical composition, and cloud forming potential of particulate emissions from a marine diesel engine at various load conditions, *Environ. Sci. Technol.*, *44*(10), 3800–3805.

Prabhakar, G., B. Ervens, Z. Wang, L. C. Maudlin, M. M. Coggon, H. H. Jonsson, J. H. Seinfeld, and A. Sorooshian (2014), Sources of nitrate in stratocumulus cloud water: Airborne measurements during the 2011 E-PEACE and 2013 NiCE studies, *Atmos. Environ.*, *97*, 166–173.

Rudich, Y., O. Khersonsky, and D. Rosenfeld (2002), Treating clouds with a grain of salt, *Geophys. Res. Lett.*, *29*(22), 2060, doi:10.1029/2002GL016055.

Russell, L. M., et al. (2013), Eastern Pacific Emitted Aerosol Cloud Experiment, *Bull. Am. Meteorol. Soc.*, *94*(5), 709–729.

Sorooshian, A., F. J. Brechtel, Y. L. Ma, R. J. Weber, A. Corless, R. C. Flagan, and J. H. Seinfeld (2006), Modeling and characterization of a particle-into-liquid sampler (PILS), *Aerosol Sci. Technol.*, *40*(6), 396–409.

Sorooshian, A., Z. Wang, G. Feingold, and T. S. L'Ecuyer (2013a), A satellite perspective on cloud water to rain water conversion rates and relationships with environmental conditions, *J. Geophys. Res. Atmos.*, *118*, 6643–6650, doi:10.1002/jgrd.50523.

Sorooshian, A., Z. Wang, M. M. Coggon, H. H. Jonsson, and B. Ervens (2013b), Observations of sharp oxalate reductions in stratocumulus clouds at variable altitudes: Organic acid and metal measurements during the 2011 E-PEACE campaign, *Environ. Sci. Technol.*, *47*(14), 7747–7756.

Szumowski, M. J., R. M. Rauber, and H. T. Ochs III (1999), The microphysical structure and evolution of Hawaiian rainbands. Part III: A test of the ultragiant nuclei hypothesis, *J. Atmos. Sci.*, *56*, 1980–2003.

Wang, Z., A. Sorooshian, G. Prabhakar, M. M. Coggon, and H. H. Jonsson (2014), Impact of emissions from shipping, land, and the ocean on stratocumulus cloud water elemental composition during the 2011 E-PEACE field campaign, *Atmos. Environ.*, *89*, 570–580.

Winnes, H., and E. Fridell (2009), Particle emissions from ships: Dependence on fuel type, *J. Air Waste Manage.*, *59*(12), 1391–1398.

Wonaschütz, A., et al. (2013), Hygroscopic properties of smoke-generated organic aerosol particles emitted in the marine atmosphere, *Atmos. Chem. Phys.*, *13*(19), 9819–9835.

Yin, Y., Z. Levin, T. G. Reisin, and S. Tzivion (2000), The effects of giant cloud condensation nuclei on the development of precipitation in convective clouds—A numerical study, *Atmos. Res.*, *53*(1–3), 91–116.